

## Copper Oxide Nanoparticles suppress the liver and kidney function and decrease antioxidant defense in adult male rats after acute oral administration

Rehab Mohamed<sup>1</sup>, Ibrahim M. A. Hasan<sup>2</sup>, Zainab M. Maher<sup>3</sup> and Hassan Ahmed<sup>1\*</sup>

<sup>1</sup>Department of Physiology, Faculty of Veterinary Medicine, South Valley University, Qena 83523, Egypt, <sup>2</sup>Department of Chemistry, Faculty of Science, South Valley University, Qena 83523, Egypt, <sup>3</sup>Department of Pathology and clinical pathology, Faculty of Veterinary Medicine, South Valley University, Qena 83523, Egypt.

### Abstract

Copper oxide nanoparticles (CuO NPs) were green synthesized using the aqueous extract of banana peels. CuO NPs were characterized by X-ray diffraction (XRD), Fourier transform infrared (FTIR) spectroscopy, transmission electron microscopy (TEM), Brunauer-Emmett-Teller (BET) surface area analysis. Analyses confirmed the formation of crystalline CuO with 15 nm particle size and 9 m<sup>2</sup>g<sup>-1</sup> surface area. The current study is an endeavor to explore the *in vivo* impact of acute different oral doses of the synthesized CuO NPs. One hundred and fifty adult male albino rats were used, they divided into 5 groups, each group contained 3 replicates (n = 30). Rats were administered suspension of CuO NPs using oral gavage in different concentrations (0, 100, 200, 1000, and 2000 mg/kg) as a single dose. Liver and kidney function markers (AST, ALP, ALP, urea and creatinine) as well as antioxidant enzymes (catalase and glutathione reductase) were evaluated 2, 8 and 15 days after administration. The results revealed a high mortality rate with rats receiving 1000 and 2000 mg/kg (16% and 30.7%, respectively). Further, within the same high doses, rats showed marked elevation of serum AST, ALP, ALP, urea and creatinine after 2, 8 and 15 days from administration. However, the activity of catalase enzyme declined significantly at the same timepoints with the former high doses. Moreover, the activity of glutathione reductase enzyme in the liver homogenate showed marked decrease after administration of all CuO NPs doses. In conclusion, the harmful effect of CuO NPs appears with the higher dose so, attention should be considered during use of CuO NPs as nutritive supplements.

**Keywords:** CuO nanoparticles, ALT, AST, catalase, glutathione reductase, oxidative distress.

DOI: 10.21608/SVU.2023.218969.1279 Received: June 20, 2023 Accepted: August 01, 2023

Published: August 19, 2023

\*Corresponding Author: Hassan Ahmed

E-mail: Hassan-younes@vet.svu.edu.eg

Citation: Mohamed et al., Copper Oxide Nanoparticles suppress the liver and kidney function and decrease antioxidant defense in adult male rats after acute oral administration. SVU-IJVS 2023, 6(3): 93-113.

Copyright: © Mohamed et al. This is an open access article distributed under the terms of the creative common attribution license, which permits unrestricted use, distribution and reproduction in any medium provided the original author and source are created.

Competing interest: The authors have declared that no competing interest exists.



## Introduction

In the last decades, nanotechnology has been considered a revolutionary field concerning characterization and application of nanomaterials, biology and chemistry. The unique-size dependent properties make these materials superior and indispensable in cellular activity. Living bodies are built of cells with typical size 10  $\mu\text{m}$  and size comparison between cellular and nanoparticles (NPs) gives an indication of the pivotal importance of these particles on cellular machinery without impairment (Taton, 2002). Hence, figuring out the biological effect of NPs on the cellular level is a strong driving force behind development of nanotechnology. However, the biological role of NPs on living cells is mainly affected by physicochemical properties such as size, surface charge and shape which are considered mainspring for cellular uptake and biodistribution of these NPs (Kim et al., 2009). For instance, NPs with size of 20 nm can cross the blood retinal barrier and can be used as therapeutic agent in retinal toxicity (Kim et al., 2009). Further, cellular uptake is the most prominent with <50 nm sized NPs (Chithrani et al., 2006). Moreover, positively charged NPs are more uptake by living cells, effectively biodistributed and interacted with other biological factors than neutral and negative ones (Schipper et al., 2009; Usman et al., 2013).

Copper oxide nanoparticles (CuO NPs) have considerable attention as it is semiconductors with unique optical, electrical, and magnetic characteristics consequently, it used for different purposes including sensors, catalysis, and semiconductors (Dagher et al., 2014). Additionally, nano-sized copper particles are useful in pharmaceutical industry because of its anti-microbial, anti-

inflammatory, and anti-fungal properties (Usman et al., 2013). However, prolonged exposure to CuO NPs contributes to biological toxicity as shown by El Bialy et al. (2020) who found that CuO NPs toxicity results in biochemical changes such as leukocytosis, elevated serum activities of alanine aminotransferase (ALT) and aspartate aminotransferase (AST) and serum levels of urea and creatinine. Besides, apoptotic effect represented by increased P53 mRNA and caspase-3 protein expressions in hepatic tissues. Moreover, CuO NPs induced degenerative and necrotized changes in hepatic, renal and splenic tissues. Further, high dose of CuO NPs enhanced generation of Reactive Oxygen Species (ROS) resulting in oxidative stress by lowering the antioxidants such as SOD and catalase levels (Anreddy, 2018). Notably, oxidative stress is considered the main accused inflammation, cytotoxicity and DNA damage by oxidation of nucleic acids followed by mitochondrial dysfunction and cell death (He et al., 2020).

The current study is an attempt to investigate the impact of acute exposure to CuO NPs in 4 different single doses (100, 200, 1000 and 2000 mg/kg) on hepato-renal function parameters, antioxidant markers and histological examination in adult male albino rats.

## Materials and methods

### Approval and registration

The protocols for animals' study were approved by the ethical research Committee of the Faculty of Veterinary Medicine, South Valley University (approval number: 26/16/11.2021), and the animals were cared for in accordance with the Egypt National Institutes of Health

Guidelines for the Care and Use of Laboratory Animals. The animals were examined and adapted to the new environmental conditions for a week before the formal experiment.

### Chemicals and reagents

All chemicals are analytical grade: copper (II) acetate monohydrate  $\text{Cu}(\text{CH}_3\text{CO}_2)_2 \cdot \text{H}_2\text{O}$  (98% purity) (Cat NO. 102710) and sodium hydroxide (99% purity) (Cat. NO.106469), purchased from Merck (Merck KGaA, Darmstadt, Germany), and used as received. Banana (*Musa acuminata*) was bought from a local market. The solutions in this experiment were made from double-distilled (DD) water.

### Preparation of banana peel extract (BPE)

Banana peels were cleaned with tap water, rinsed with distilled water and dried for 15 days under sunlight. Twenty grams of dried banana peels were boiled for 15 minutes in 300 mL distilled water in a Pyrex glass beaker and then left at room temperature overnight. The mixture was doubly filtered using a blog of glass wool in the first step and Whatman No. 1 filter paper in the second step. The extract was stored at 4 °C until use.

### Synthesis and characterization of copper oxide nanoparticles (CuO NPs)

Synthesis was carried out according to our previous method with some

modifications (Hasan et al., 2021; Hasan et al., 2022) and is shown schematically in scheme 1. Five grams of  $\text{Cu}(\text{CH}_3\text{CO}_2)_2 \cdot \text{H}_2\text{O}$  were added to 60 mL BPE (1:12 m/v) under stirring and heating for 5 min. Then, 60 mL 5 % NaOH was added to the reaction mixture in portions and the reaction was continued further for 30 min when the black CuO was completely precipitated. The CuO NPs were isolated through centrifugation at 6,000 rpm for 12 min followed by washing by DD H<sub>2</sub>O and ethanol three times each and drying at 80°C for 3 hours. The resulting product was crushed using pestle and mortar and stored in a sealed container.

The synthesized CuO NPs were characterized for phase structure and size analysis using powder x-ray diffractometer (X'Pert3 Powder, PANalytical, The Netherlands) which was operated at 40 kV voltage and 30 mA current, using monochromatic radiation (Cu-K $\alpha$ , 1.5406 Å) with diffraction angle in the 20-80° range. The crystallite size was determined using Scherrer equation ( $D = K\lambda/\beta\cos\theta$ ). To evaluate the possible role of phytochemicals in the synthesis of CuO NPs, FTIR spectra were taken from 400-4000  $\text{cm}^{-1}$  (Shimadzu FTIR, Kyoto, Japan). The size and shape of CuO NPs was checked by TEM analysis.



Scheme 1: Green synthesis of CuO NPs

### **Experimental animals**

One-hundred and fifty adult male apparently clinically healthy albino rats (Wistar strain) weighing 150 to 250 g and aged from 12 to 14 weeks were obtained from the animal house of the Faculty of Medicine, Assiut University, Assiut, Egypt. The animals were transferred to animal house, Department of Physiology, Faculty of Veterinary Medicine, South Valley University, Qena, Egypt. Rats were housed in clean plastic cages under normal healthy conditions (23-25°C, 40-70% humidity, and with 12-h light/12-h dark cycles), and they were kept under observation before the start of the experiment for a week. A standard rat chow diet and tap water were available ad libitum. Cages, bedding, and glass water bottles were changed once or twice per week.

### **Experimental design**

The experimental period lasted for 15 days, after a week of the acclimatization period, the rats were randomly divided into five different groups, each group subdivided into 3 subgroups (n = 30, 10 rats per subgroup). The rats were assigned to specific treatments with the following doses according to OECD (2001):

Control group (I): Rats received deionized water at a dose 1 ml/kg body weight (BW) orally administered with oral gavage at a single dose.

Group II (100 mg/kg): Rats received 100 mg/kg BW from CuO NPs orally administered with oral gavage at a single dose.

Group III (200 mg/kg): Rats received 200 mg/kg BW from CuO NPs orally administered with oral gavage at a single dose.

Group IV (1000 mg/kg): Rats received 1000 mg/kg BW from CuO NPs orally

administered with oral gavage at a single dose.

Group V (2000 mg/kg): Rats received 2000 mg/kg BW from CuO NPs orally administered with oral gavage at a single dose.

Dry powder of CuO NPs was suspended in deionized water then sonicated at room temperature for 10 min to form a homogeneous suspension. The time interval from preparation to oral gavage was limited to 20 min to ensure that the NPs will not be aggregated before administration. All rats were dosed orally using oral gavage with a dosing volume of 10 mL/kg body weight.

### **Recording of mortality rates**

Along the experimental period, animals were checked twice a day for mortality rates during the experimental period. In addition, the dead rats were dissected, and all organs were examined for post-mortem changes.

### **Blood samples collection**

After the end of experimental time, one subgroup (10 rats) from each treated group were sedated with diethyl ether at 2, 8 and 15 days after deionized water or CuO NPs administration. Blood samples were collected from the retro-orbital venous plexus and centrifuged at 3000 rpm for 15 minutes and sera were stored at -80°C until the evaluation of liver and kidney function parameters (AST, ALT, ALP, urea and creatinine) and antioxidant markers (Catalase and glutathione reductase enzymes).

### **Biochemical estimation**

The level of liver and kidney function parameters (AST, ALT, ALP, urea and creatinine; Cat. NO. AS 10 61, AL 10 31, AP 10 20, UR 21 10 and CR 12 51, respectively) as well as antioxidant markers (catalase and glutathione reductase, Cat. NO. CA 25 17 and GR 25 23, respectively)

were determined in the serum by colorimetric method (Spectrophotometry) using specific kits according to manufacturer's instructions (Biomed Diagnostics, Badr city, Egypt) by spectrophotometer T80 UV/VIS spectrophotometer (PG Instruments, UK).

### **Histological examination**

At the end of the experiment, rats were anesthetized with an intraperitoneal injection of sodium thiopental (50 mg/kg bw) then one subgroup from each group was sacrificed at 2, 8 and 15 days CuO NPs administration. The specimens of liver and kidney tissues were rapidly removed (Kittel et al., 2004), fixed in 4% neutral buffered paraformaldehyde, processed through the conventional paraffin embedding technique then sectioned at approximately 5  $\mu$ m thick. Tissue sections will be stained with Hematoxylin and Eosin (H&E) (Gamble, 2008) and examined under a light microscope for any alteration of normal histological structure.

#### **1. Data analysis and statistics**

Results were analyzed statistically by Graph pad prism 8 (GraphPad Software, San Diego, California USA). Data were expressed as mean  $\pm$  standard error of mean (SEM) and differences between groups will be analyzed by using Two-way analysis of variance (ANOVA) followed by Tukey's multiple comparisons test. Values of  $P < 0.05$  were considered significant compared with control.

## **Results**

### **Characterization of CuO NPs**

Figure 1A shows the XRD of the green synthesized CuO NPs to identify the phase and crystal structure. The sample showed

several diffraction peaks characteristic of the crystalline nanoparticles at 2 $\theta$  values of 32.48, 35.63, 38.86, 48.84, 53.27, 58.39, 61.55, 66.35, 68.23, 72.63, 74.35, and 82.71 corresponding to respective Miller indices of (110), (11-1), (200), (20-2), (020), (202), (-113), (310), (220), (221), (004) and (222). These values were well matched with COD file no. 9016326 (Asbrink and Waskowska, 1991) (volume-81.5, system-monoclinic, space group- C 1 c 1 (9), cell parameter a = 4.6927, b = 3.4283, c = 5.137, a/b = 1.36881, c/b = 1.49841). The CuO NPs have an average crystallite size of 14.50 nm using Scherrer equation (Table 1).

FTIR spectroscopy investigations were used to determine the involvement of phytochemicals in the BPE extract in the reduction of copper salt and capping of the resulting nanoparticles. Absorption peaks in the wavenumber region of 400 to 4000  $\text{cm}^{-1}$  are visible in comparison FTIR spectra (Figure 1B).

The BPE FTIR spectrum contained major peaks in the range of 3418 and 1623  $\text{cm}^{-1}$ . These peaks are attributed to O-H stretching and the in-plane bending vibrations of hydroxyl groups or possible stretching of the N-H group of amides. The peaks at 2931 and 1055  $\text{cm}^{-1}$  point to C-N (unsaturated) and C-H bending vibration, respectively. The spectrum of CuO NPs (Figure 1B) displayed peaks at 3426, and 1632  $\text{cm}^{-1}$  indicating the OH stretching and OH bending, respectively. Besides, the characteristic Cu-O peaks were noticed at 632 and 539  $\text{cm}^{-1}$  (Maulana et al., 2022; Vinothkanna et al., 2022). These results confirm the reducing and capping actions of organic moieties in BLE.

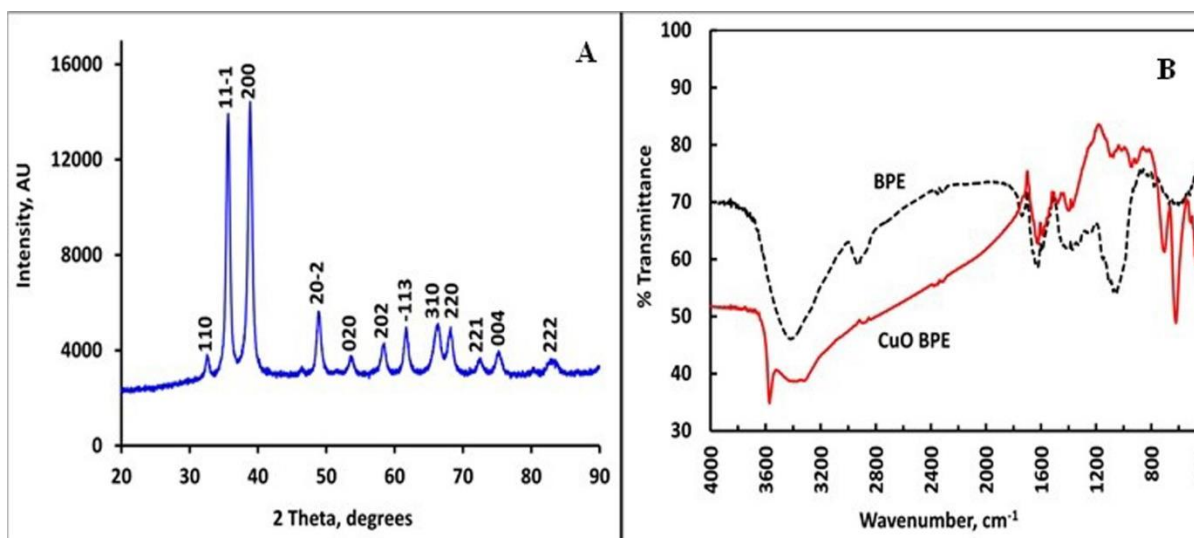


Figure 1: (A) XRD of CuO NPs and (B) FTIR spectra of BPE and green synthesized CuO NPs.

The morphology of the as-synthesized CuO NPs was studied by TEM (Figure 2A). The image shows the spherical CuO NPs aggregates with an average particle size of

15 nm (Table 1). The selected area electron diffraction (SAED) pattern (Figure 2B) reveals the crystalline nature of the CuO NPs.

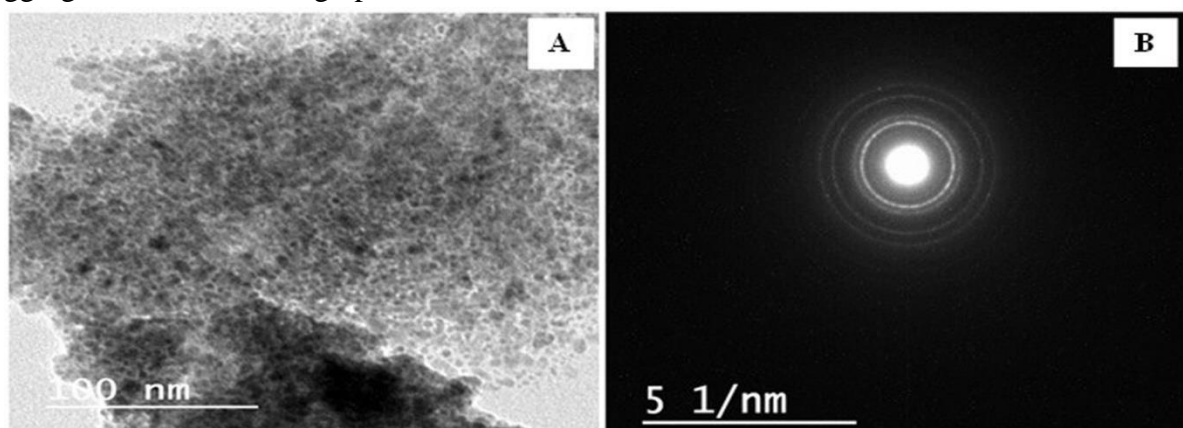


Figure 2: (A) TEM image and (B) SAED pattern of CuO NPs.

The physicochemical activity is affected by the material surface area, where the reactions occur. The higher surface area normally corresponds to higher activity. The Brunauer-Emmett-Teller (BET) surface area and the Non-Local Density Functional Theory/Grand Canonical Monte Carlo (NLDFT/GCMC) pore size of the CuO NPs have been investigated using N<sub>2</sub> adsorption/desorption analysis at 77 K. According to the IUPAC classification, the N<sub>2</sub> sorption isotherm of CuO NPs at P/P<sub>0</sub> = 0.982 (Figure 3A) is classified as Type IV

with a single point final plateau and a Type H3 hysteresis loop, which refers to non-rigid aggregates of mesoporous particles leading to slit-shaped pores (Thommes et al., 2015). Moreover, the mean pore diameter is 8.9135 nm as calculated by the NLDFT/GCMC pore size distribution curve (Figure 3B) confirming the mesoporous structure of CuO NPs. Adopting a 16.2 Å for the cross-section area of the N<sub>2</sub> molecule, the calculated BET specific surface area is 8.839. Additionally, the total pore volume at saturation pressure is 0.0197

cm<sup>3</sup> g<sup>-1</sup> according to both BET and NLDFT/GCMC (Table 1).

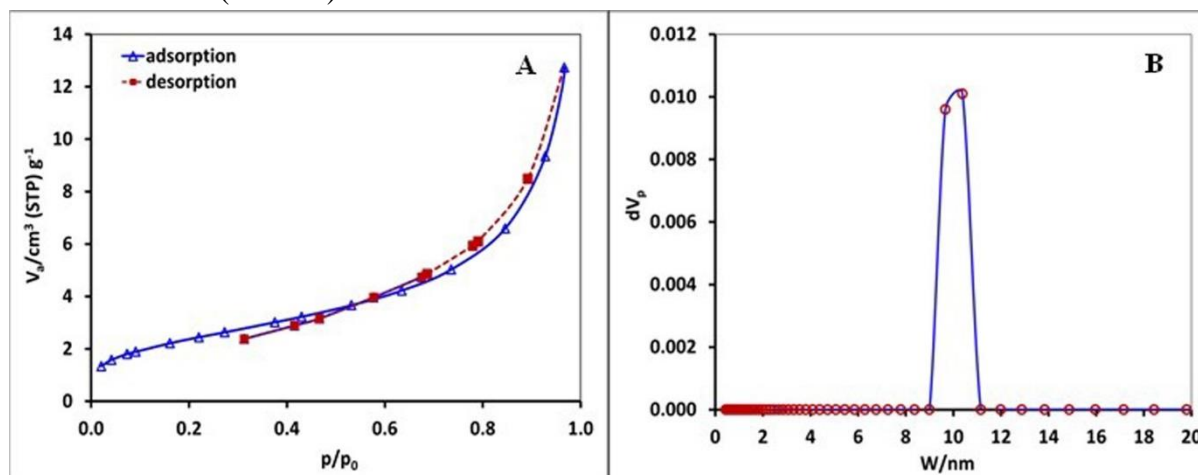


Figure 3: (A) Adsorption/desorption isotherm and (B) NLDFT/GCMC pore size distribution analysis of CuO NPs.

Table 1: Physical characteristics of the synthesized CuO NPs

Sample	Crystallite size (XRD)	Crystallite size (TEM)	Surface area	Mean pore diameter	Pore volume, cm <sup>3</sup> g <sup>-1</sup>	
					BET	NLDFT
CuO BPE	14.50 nm	15.0 nm	8.839 m <sup>2</sup> g <sup>-1</sup>	8.9135 nm	0.0197	0.0197

**Elevated mortality rate is associated with high dose of CuO NPs acute exposure**

The mortality rate of the experimental rats was recorded in control and treated groups during the experimental period after a single dose of CuO NPs administration as shown in figure 4. After 2 days from administration, the highest mortality percent was 19.23 % in rats received 2000 mg/kg BW and the percentage elevated in

the same group after 8 and 15 days to reach 23.07 % and 30.77 %, respectively.

However, the death percent in other groups was lower than that in 2000 mg/kg-treated rats, for instance rats administered 1000 mg/kg showed mortality percent 8 and 16 % after 8 and 15 days from CuO NPs administration, respectively. Further, Rats treated with 200 and 100 mg/kg showed lower mortalities only after 15 days in percent 3.85 and 7.14%, respectively.

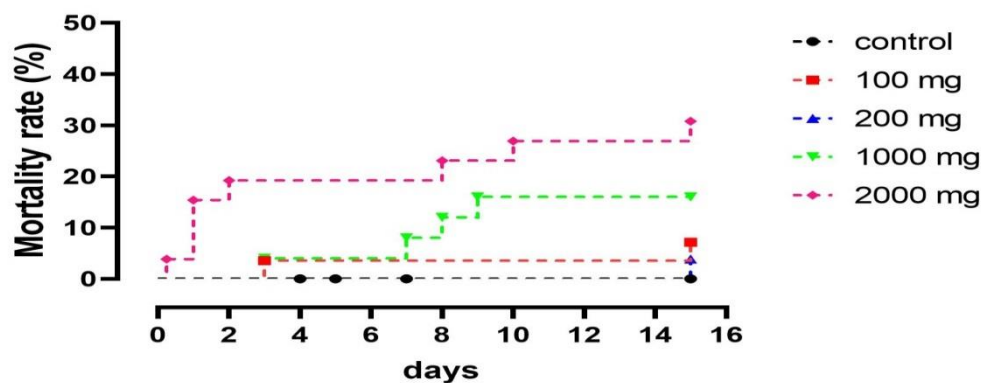


Figure 4: Mortality rates of different treated rats' groups during experimental period. Values expressed as a percentage (%) of dead rats compared with the initial group (n = 26).

### Oral administration of CuO NPs adversely elevated serum AST, ALT and ALP level

Figure 5 illustrates serum AST (Units/mL), ALT (Units/mL) and ALP (IU/L) in control and treated rats after 2, 8 and 15 days from CuO NPs administration. After 2, 8 and 15 days from administration, rats received 100 and 200 mg/kg showed non-significant increase in serum AST (161.97±15.47, 171.61± 7.81 and 148.50±13.29, respectively in 100 mg-treated group and 167.44±6.35, 175.16±8.44 172.11±13.15, respectively in 200 mg-treated group) compared with the corresponding control (145.38±6.86, 154.88±11.61 and 148.50±13.29, respectively).

Similarly, non-significant elevation of serum AST appeared 2 and 8 days (189.75±11.88 and 194.53±14.91, respectively in 1000 mg-treated group and 195.51±15.50 and 200.07±12.09, respectively in 2000 mg-treated group) compared with the control, 100 and 200 mg treated groups.

However, the deleterious effect of CuO NPs markedly observed 15 days after higher dose administration (1000 and 2000 mg/kg). Treated rats disclosed a significance ( $P < 0.05$ ) increase (199.14 ± 15.58 and 198.76 ± 11.04, respectively) in serum AST compared with corresponding control (148.50 ± 13.29) and non-significant increase compared with 100 and 200 mg-treated groups in the same timepoint as shown in figure 5 A.

The adverse effect of CuO NPs administration appeared clearly on serum ALT level as 100 and 200 mg/kg-treated rats showed non-significant increase after 2 days (58.19±4.05 and 54.28±3.21, respectively) compared with control (42.27±2.80), 8 days (61.66±3.17 and

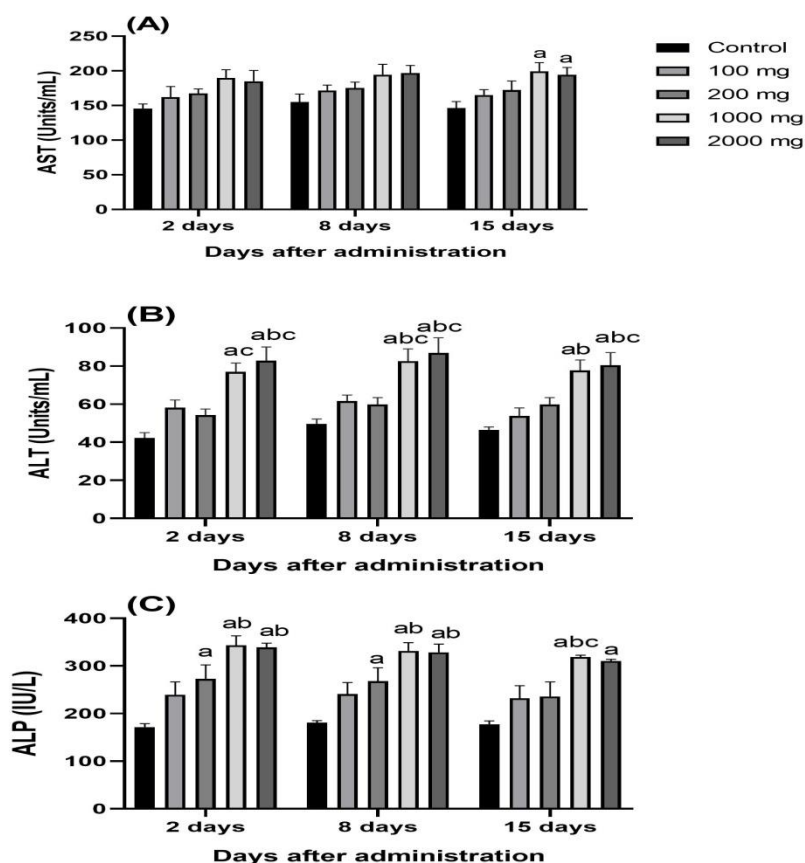
59.79±3.64, respectively) compared with control (49.64±2.54) and 15 days (53.77±4.28 and 56.37±4.14, respectively) compared with control (45.75±1.71). In addition, rats that received 1000 mg disclosed a significant ( $P < 0.05$ ) increase in serum ALT level (76.99±4.62) after 2 days compared with control and 200 mg groups, (82.60±6.41) after 8 days compared with control, 100 and 200 mg groups and (77.73±6.68) after 15 days compared with control and 100 mg groups. Likewise, rats treated with 2000 mg/kg CuO NPs denoted significant ( $P < 0.05$ ) increase in serum ALT level after 2, 8 and 15 days from administration (82.89±8.50, 86.96±7.94 and 80.42 ±6.72, respectively) compared with control, 100 and 200 mg groups (Figure 5B).

Figure 5C illustrates the serum level of ALP in the control and treated rats after 2, 8 and 15 days from administration. After 2, 8 and 15 days, rats treated with 100 mg showed non-significant elevation (239.51±26.88, 241.14±24.00 and 232.04±26.58, respectively) of serum ALP compared with corresponding control (171.49±7.45, 180.84±4.32 and 175.64

9.80, respectively). However, rats received 200 mg/kg CuO NPs showed significant ( $P < 0.05$ ) increase in serum ALP level after 2 and 8 days from administration (272.80±29.38 and 268.30±27.96, respectively) compared with the control (171.49±7.45 and 180.84±4.32, respectively) while after 15 days ALP elevated (235.75±30.8) non-significantly compared with control (175.64±9.80). However, the alteration effect of CuO NPs markedly observed in high doses-treated groups (1000 and 2000 mg/kg). After 2 and 8 days from administration, ALP level elevated significantly ( $P < 0.05$ ) in 1000 mg- (343.56±19.61 and 331.35±17.45,

respectively) and 2000 mg-treated groups ( $339.07 \pm 10.26$  and  $328.55 \pm 17.15$ , respectively) compared with control and 200 mg-treated rats. Further, after 15 days from administration, rats treated with 1000 mg/kg showed significant ( $P < 0.05$ ) increase in ALP level ( $318.76 \pm 4.71$ )

compared with control, 100 and 200 mg/kg groups. Also, those treated with 2000 mg/kg showed significant ( $P < 0.05$ ) elevation in ALP level ( $312.56 \pm 4.43$ ) compared with control group and non-significant increase compared with 100 and 200 mg-treated groups.



**Figure 5: Serum level of AST (Units/mL) (A), ALT (Units/mL) (B), and ALP (IU/L) (C) in control and treated rats after 2, 8 and 15 days from CuO NPs administration.**

Data are expressed as the mean  $\pm$  SEM ( $n = 3-5$ , Two-way ANOVA) <sup>a</sup> $P < 0.05$ , vs. Control, <sup>b</sup> $P < 0.05$ , vs. 100 mg, and <sup>c</sup> $P < 0.05$ , vs. 200 mg.

### Circulating urea and creatinine level increased after CuO NPs administration

Figure 6 discloses the serum urea (mg/dL) and creatinine (mg/dL) levels in all experimental rats at 2, 8 and 15 days after oral administration of CuO NPs. Two days after administration, rats treated with 100, 200 and 1000 mg/kg showed non-significant elevation in urea level ( $68.56 \pm 5.78$ ,  $72.85 \pm 4.36$  and  $93.85 \pm 16.08$ , respectively) compared with control ( $43.62 \pm 2.53$ ). However, the highest dose (2000 mg/kg) showed significant ( $P < 0.05$ ) increase in urea level ( $128.68 \pm 14.79$ ) compared with control, 100- and 200-treated groups and non-significantly

compared with 1000 mg-treated rats. Moreover, after 8 and 15 days from administration, rats treated with 100 and 200 mg/kg disclosed non-significant elevation in urea level ( $78.72 \pm 28.48$  and  $80.85 \pm 5.11$ , respectively in 100 mg group;  $87.77 \pm 15.62$  and  $91.17 \pm 6.36$ , respectively in 200 mg group) compared with control ( $51.79 \pm 4.04$  and  $49.57 \pm 7.81$ , respectively). Whilst rats treated with 1000 and 2000 mg/kg disclosed significant ( $P < 0.05$ ) elevation in urea level ( $103.85 \pm 14.59$  and  $107.00 \pm 5.91$ , respectively in 1000 mg group;  $132.98 \pm 17.08$  and  $130.78 \pm 20.31$ ,

respectively in 2000 mg group) compared with control and non-significantly compared with 100 and 200 mg-treated groups. (Figure 6A).

Similarly, creatinine levels revealed different degrees of elevation in dose-dependent manner. For instance, 100- and 200- mg/kg treated groups showed non-significant increase in creatinine level ( $68.56 \pm 5.78$  and  $72.85 \pm 4.36$ , respectively) after 2 days, ( $78.72 \pm 28.48$  and  $87.77 \pm 15.62$ , respectively) after 8 days and ( $80.85 \pm 5.11$  and  $91.17 \pm 6.36$ , respectively) after 15 days compared with the corresponding control ( $43.62 \pm 2.53$ ,  $51.79 \pm 4.04$  and  $49.57 \pm 7.81$ , respectively). Furthermore, rats treated with 1000 mg/kg revealed non-significant increase in

creatinine level ( $93.85 \pm 16.08$ ) after 2 days from administration and significant ( $P < 0.05$ ) elevation after 8 and 15 days ( $103.85 \pm 14.59$  and  $107.00 \pm 5.91$ , respectively) compared with the corresponding control. Besides, after administration of 2000 mg/kg of CuO NPs, rats showed significant ( $P < 0.05$ ) increase in creatinine level ( $128.68 \pm 14.79$ ) after 2 days compared with control, 100 and 200 mg/kg groups. In addition, the same group disclosed significant ( $P < 0.05$ ) elevation in creatinine level after 8 and 15 days ( $132.98 \pm 17.08$  and  $130.78 \pm 20.31$ , respectively) compared with the corresponding control and non-significantly compared with 100 and 200 mg-treated groups. (Figure 6B).

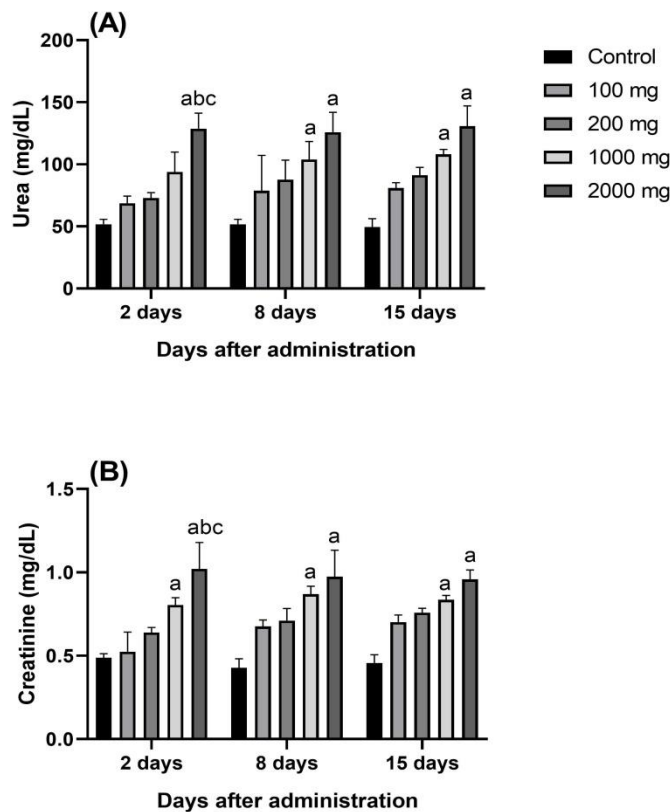


**Figure 6: The serum urea (A) and creatinine (B) levels at different time points (2, 8 and 15 days) after the oral administration of CuO NPs in control and treated groups. Data are expressed as the mean  $\pm$  SEM ( $n = 3-5$ , Two-way ANOVA) <sup>a</sup> $P < 0.05$ , vs. Control, <sup>b</sup> $P < 0.05$ , vs. 100 mg, and <sup>c</sup> $P < 0.05$ , vs. 200 mg.**

### Alteration of antioxidant status after acute oral administration of CuO NPs

Serum catalase and glutathione reductase level (U/L) was evaluated in all experimental rats at 2, 8, and 15 days after CuO NPs administration as clarified in figure 7. Serum catalase level disclosed non-significant decrease after 2, 8, and 15 days in 100- mg/kg treated group ( $399.79 \pm 42.39$ ,  $376.23 \pm 45.13$  and  $365.37 \pm 27.25$ , respectively) as well as 200- mg/kg treated group ( $346.76 \pm 46.91$ ,  $334.11 \pm 26.94$  and  $316.59 \pm 37.13$ , respectively) compared with control ( $446.71 \pm 64.46$ ,  $459.46 \pm 28.30$  and  $453.32 \pm 36.90$ , respectively). In addition, administration of 1000 mg/kg CuO NPs induced significant ( $P < 0.05$ ) decline of serum catalase level after 2, 8, and 15 days ( $293.61 \pm 45.49$ ,  $269.91 \pm 51.60$  and  $271.97 \pm 41.55$ , respectively) compared with control and non-significantly compared with 100 and 200 mg-treated groups. Furthermore, administration of 2000 mg/kg

CuO NPs initiated a significant ( $P < 0.05$ ) reduction in serum catalase level ( $185.78 \pm 22.31$ ) after 2 days compared with control, 100- and 200 mg/kg treated rats. In addition, at 8 and 15 days the same group showed a significant ( $P < 0.05$ ) decrease in serum catalase level ( $199.91 \pm 15.27$  and  $189.61 \pm 18.55$ , respectively) compared with the control and 100- mg/kg treated rats and non-significantly compared with 200 and 1000 mg-treated groups. (Figure 7A).

Constantly, Serum glutathione reductase level decreased significantly ( $P < 0.05$ ) in 100-, 200-, 1000- and 2000- mg/kg treated groups after 2 days ( $10.92 \pm 1.71$ ,  $9.45 \pm 1.10$ ,  $7.26 \pm 1.07$  and  $6.55 \pm 0.56$ , respectively), 8 days ( $8.02 \pm 0.98$ ,  $8.89 \pm 1.94$ ,  $7.69 \pm 0.48$  and  $5.54 \pm 0.44$ , respectively) and 15 days ( $11.72 \pm 1.60$ ,  $9.33 \pm 1.25$ ,  $7.13 \pm 1.17$  and  $6.94 \pm 0.65$ , respectively) compared with corresponding control ( $10.92 \pm 1.71$ ,  $18.39 \pm 3.49$  and  $16.59 \pm 1.21$ , respectively) (figure 7B).

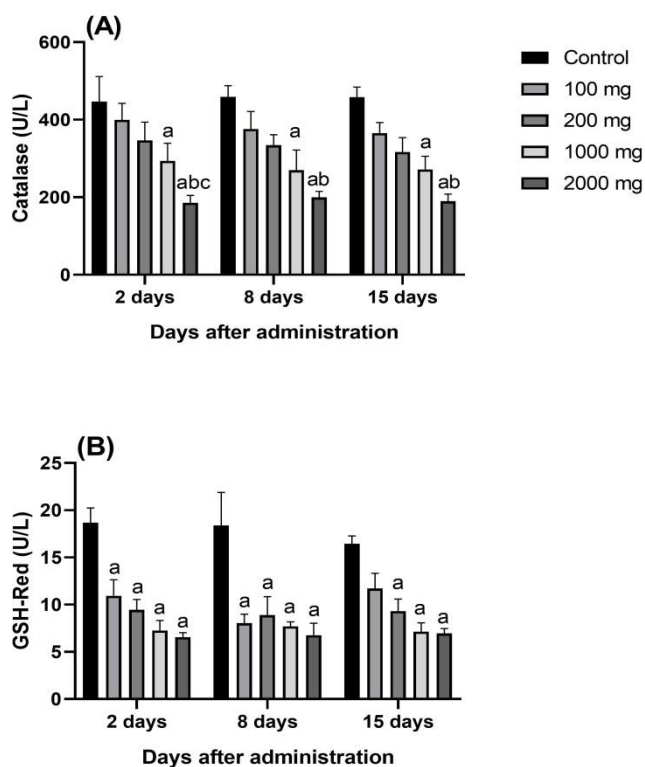


**Figure 7: The serum catalase (A) and glutathione reductase (B) levels at different time points (2, 8 and 15 days) after the administration of CuO NPs in control and treated groups. Data are expressed as the mean  $\pm$  SEM ( $n = 3-5$ , Two-way ANOVA) <sup>a</sup> $P < 0.05$ , vs. Control, <sup>b</sup> $P < 0.05$ , vs. 100 mg, and <sup>c</sup> $P < 0.05$ , vs. 200 mg.**

### **Alteration of hepatic histological architecture after CuO NPs oral administration**

The liver tissue samples were collected at 2, 8 and 15 days after deionized water or CuO NPs oral administration and immediately processed for histopathological examination under a light microscope. The microscopical examination of liver tissue of the control group (Figure 8A-C) which showed normal histological architecture represented by hepatic lobule composed of central vein surrounded by hepatocytes with abundant granular eosinophilic cytoplasm, centrally placed round to ovoid nuclei. Besides, blood sinusoids were located between the hepatocytes and lined with Kupffer cells. On contrary, the former hepatic histological structure was disturbed by CuO NPs in dose and time dependent manner. Two days after 100 mg/kg CuO NPs were administered, hepatic tissue showed mild dilatation of ventral vein with moderate hepatocyte necrosis with inflammatory cells infiltration. The same changes appeared after 8 and 15 days of administration in addition to hemosiderosis and Kupffer cell aggregation (Figure 8D-F). Likewise, rats treated with 200 mg/kg CuO NPs showed mild vascular degeneration and hepatocyte degeneration after 2, 8 and 15 days (Figure

### **Adverse renal histological change induced by CuO NPs oral administration**

The kidney tissue specimens were harvested from the control and treated groups after 2, 8 and 15 days and processed for histopathological examination. Figure 9A-C showed normal renal histological structure with renal corpuscles and glomerulus surrounded by Bowman's space. Furthermore, proximal and distal convoluted tubules were lined with cuboidal cells with rounded nuclei.

8G-I). However, higher dose of CuO NPs (1000 mg/kg) disclosed marked alteration in hepatic tissue represented by congested and dilated central vein in addition to vacuolar degeneration and necrosis in hepatocytes after 2 days from administration. Moreover, after 8 days from administration, the hepatic tissue showed sever congestion and dilatation of the central vein, necrosis of hepatocytes besides hemosiderosis. The alteration of histological structure was worst after 15 d from administration; the hepatic tissue revealed sever congestion and dilatation of the hepatic vein, necrosis and vacuolation of hepatocytes, hemosiderosis and infiltration of inflammatory cells (Figure 8J-L). Furthermore, 2 d after oral administration of CuO NPs higher dose (2000 mg/kg) resulted in sever congestion and dilatation of central vein surrounded by vacuolated and degenerated hepatocytes. After 8 and 15 d, the adverse change in the hepatic tissue appeared with sever congestion and dilatation of central vein, necrosis of hepatocytes with vacuolated cytoplasm and pyknotic nuclei. In addition, blood sinusoids appeared dilated and congested with blood in their lumen and markedly inflammatory cells infiltration (Figure 8M-O).

However, 2, 8 and 15 d after oral administration of CuO NPs (100 mg/kg) showed mild necrosis of the glomerulus and widening of Bowman's space in addition to degeneration of tubular lining cells associated with interstitial hemorrhage (Figure 9D-F). Likewise, 2, 8 and 15 d after administration of CuO NPs 200 mg/kg, renal tissue revealed moderate necrosis of glomerulus, mild necrosis of renal tubular epithelium with few interstitial mononuclear cell infiltrations (Figure 9G-

I). Surprisingly, the adverse effect of CuO NPs higher dose on renal histological architecture was obvious after 2, 8 and 15 days from administration. Alteration of histological structure represented by sever necrosis of the glomeruli, widening of Bowman's space, sever necrosis and

desquamation of tubular lining cells. In addition, appearance of cystic dilatation in the renal tubules, interstitial hemorrhage associated with interstitial inflammatory cells infiltration after oral administration of 1000 (Figure 9J-L) and 2000 mg/kg (Figure 9M-O).

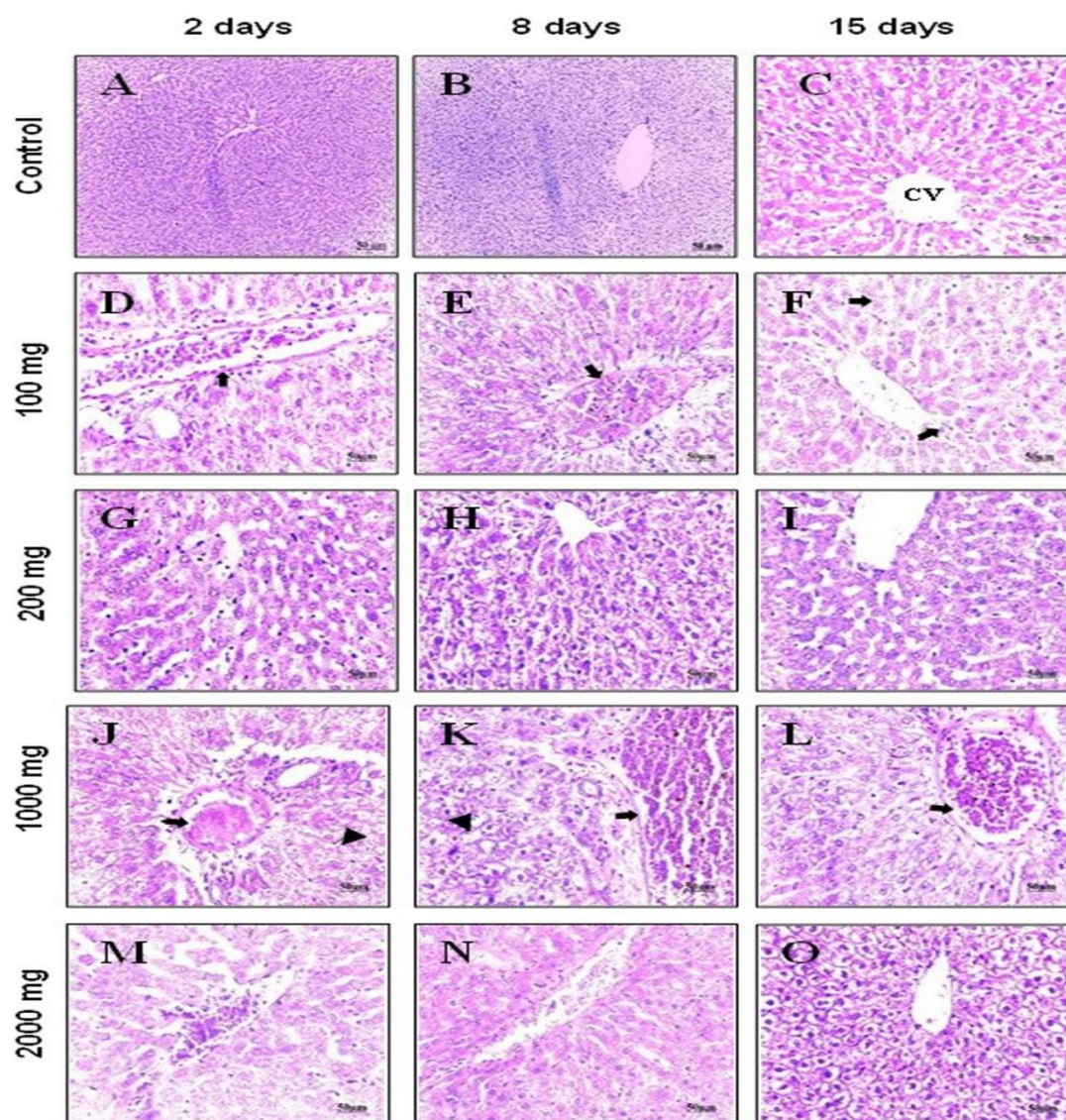


**Figure 8: Photomicrograph of the liver in control and treated groups after 2, 8 and 15 days after administration of 100, 200, 1000 and 2000 mg of CuO NPs. (A-C) Liver of control group showing normal morphology of central vein (CV) and hepatic cord. (D) Liver of 100 mg-treated group after 2 days showing mild congestion and dilation in central vein (arrow) and necrotic hepatocytes with inflammatory cells infiltration. (E) Liver of 100 mg-treated group after 8 days showing hepatocytes necrosis with dilated central vein and hemosiderosis in addition to Kupffer cell aggregation. (F) Liver of 100 mg-treated group after 15 days showing moderate necrosis in the in hepatic cells with dilated central vein and Kupffer cells infiltration (arrows). (G) Liver of 200 mg-treated group after 2 days showing mild necrosed hepatocytes. (H) Liver of 200 mg-treated group after 8 days showing vacuolar degeneration and necrosis in hepatocytes. (I) Liver of 200 mg-treated group after 15 days showing vacuolar degeneration and some necrosed hepatocytes. (J) Liver of 1000 mg-treated group after 2 days showing vacuolar degeneration and necrosis in hepatocytes (arrowhead) besides, congested and dilated central vein (arrow). (K) Liver of 1000 mg-treated group after 8 days showing sever congested and dilation in central vein vacuolar degeneration and necrosis in hepatocytes (arrowhead) and hemosiderosis**

(arrow). (L) Liver of 1000 mg-treated group after 15 days showing sever vacular degeneration and necrosis in hepatocytes besides congested and sever dilation in central vein and hemosiderosis (arrow). (M) Liver of 2000 mg-treated group after 2 days showing mild necrosed hepatocytes. (N) Liver of 2000 mg-treated group after 8 days showing sever congestion and dilatation of central vein and vaccular degeneration and necrosis in hepatocytes with pyknotic nuclei. (O) Liver of 2000 mg-treated group after 15 days showing sever congestion and dilatation of central vein with vaccular degeneration and some necrosed hepatocytes, congestion of blood sinusoid and Kupffer cells infiltration. (H&E x 400, Scale bar = 50  $\mu$ m).

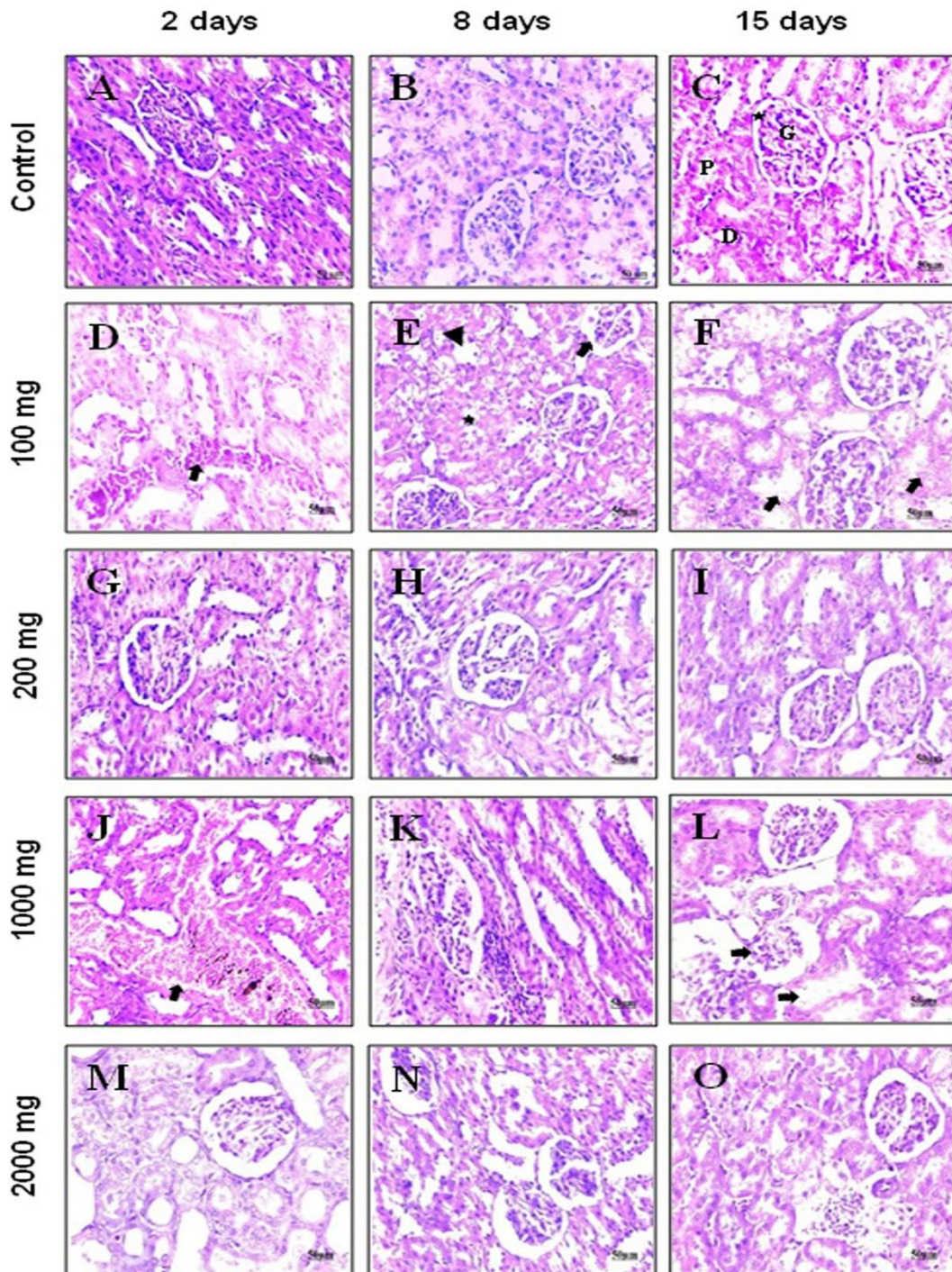


**Figure 9: Photomicrograph of the kidney in control and treated groups after 2, 8 and 15 days after administration of 100, 200, 1000 and 2000 mg of CuO NPs. (A-C) kidney of control group showing normal histological structure of the glomeruli (G), Bowman's space (Asterisks), proximal (P) and distal (D) convolute tubules. (D) kidney of 100 mg-treated group after 2 days showing necrosis in the renal tubules with sever interstitial hemorrhage (arrow). (E) kidney of 100 mg-treated group after 8 days showing necrosis in the glomeruli (arrow) and renal tubules (asterisk) with tubular cystic dilation (arrowhead). (F) kidney of 100 mg-treated group after 15 days showing sever necrosis and vacuolation in the renal tubules (arrows) with apparently normal glomeruli. (G) kidney of 200 mg-treated group after 2 days showing moderate necrosis in the renal tubular epithelium. (H) kidney**

of 200 mg-treated group after 8 days showing few interstitial mononuclear cell infiltration and moderate necrosis in renal tubules. **(I)** kidney of 200 mg-treated group after 15 days showing necrosed and cystic dilatation in renal tubules. **(J)** kidney of 1000 mg-treated group after 2 days showing sever interstitial hemorrhage with hemosiderosi and necrosis in the renal tubules (arrow). **(K)** kidney of 1000 mg-treated group after 8 days showing interstitial mononuclear cell infiltration and necrosis in the renal tubules. **(L)** kidney of 1000 mg-treated group after 15 day showing interstitial mononuclear cell infiltration and necrosed renal tubules with necrosis in the glomeru (arrows). **(M)** kidney of 2000 mg-treated group after 2 days showing sever necrosis and cystic dilatation in renal tubules. **(N)** kidney of 2000 mg-treated group after 8 days showing sever necrosis in renal glomeruli and tubule with cystic dilatation in the renal tubules. **(O)** kidney of 2000 mg-treated group after 15 days showing necrosis i renal tubules and interstitial inflammatory cells infiltration. **(H&E x 400, Scale bar = 50  $\mu$ m).**

## Discussion

The current study is an attempt to elucidate the effect of acute copper oxide nanoparticles (CuO NPs) oral administration on the liver and kidney functions as well as antioxidant status in male rats. For this purpose, single dose of CuO NPs were administered in 100, 200, 1000 and 2000 mg/kg for 15 days and liver, kidney function markers and antioxidant indicators were determined at 2<sup>nd</sup>, 8<sup>th</sup>, and 15<sup>th</sup> days of the experiment. Liver and kidney function markers (AST, ALT, ALP, urea and creatinine) were adversely affected by acute CuO NPs administration that is confirmed by deleterious change in hepatic and renal tissue histological structure. Besides, the activity of antioxidant enzymes (catalase and glutathione reductase) was reduced markedly especially with the high doses of CuO NPs.

Copper oxide nanoparticles are vastly used in electronics, semiconductors and energy storing devices. In addition, they possess a potential biomedical application such as antimicrobial, anticancer, antifungal and antibacterial agent (Grigore et al., 2016; Waris et al., 2021). Copper (Cu) is a trace element that is an essential agent in different biological activities. It is the key to energy production, erythropoiesis, synthesis of myelin, collagen and elastin, hormone synthesis and main contributor in cellular protection against oxidative stress (Osredkar and Sustar, 2011; Bhattacharya et

al., 2016). However, exposure to the overdose of copper is associated with physiological alteration and it is implicated in different diseases (Gaetke et al., 2014). Development in CuO NPs production and use increases its exposure and adverse effect on the animals and human being (S. Naz et al., 2020). Moreover, the nanoparticles have more deleterious effect than the large particles of the same compound (Lee et al., 2016). Nanoparticles have more ability to diffuse through the tissue and cellular level increasing the accumulation rate inside the cell, enhancing the reaction with cellular organelles; generating reactive oxygen species (ROS) which is the main damaging factor to the cellular biological processes (Ameh and Sayes, 2019). Furthermore, due to their extremely small size, CuO NPs easily diffuse between the cells and cross the cell membrane reaching the blood and lymph circulation and distributed to the target organs (Lee et al., 2016). It is worth mentioning that the ingestion of CuO NPs through GIT rapidly reacts with the gastric acid liberating hydrogen ions and production of ionic copper. Consequently, ionic copper deposition is markedly increased in the target organs notably liver, kidney and spleen (Chen et al., 2006).

Herein, the high mortality rate was recorded with the higher doses (1000 and 2000 mg/kg) of CuO NPs (16% and 30.7%, respectively). This is owing to the oxidative

and cellular damage induced by CuO NPs to the vital organs (Anreddy, 2018). Moreover, CuO NPs enhance immunotoxicity by impairment of phagocytic activity of the granulocyte's disturbance of oxidative/antioxidative balance (Tulinska et al., 2022).

Liver is a primary target organ for Cu deposition, the accumulation of Cu in the liver is enhanced by exposure to CuO NPs by oral route that gives the chance for liberating ionic Cu to reach liver owing to the small size of the nanoparticles enabling them to cross cell membrane easily by direct diffusion or active transport (Chen et al., 2006). Further, presence of CuO NPs inside the hepatocytes is the main cause of disturbed normal hepatic function (Lee et al., 2016). In addition, CuO NPs interact with the cell organelles especially mitochondria producing reactive oxygen species and suppressing the antioxidant enzymes ending with cytotoxicity, DNA damage and apoptosis (Lateef et al., 2023). In the present study, the disturbance of the hepatic physiological function was observed by marked elevation of serum AST, ALT and ALP particularly in the higher dose. Bugata et al. (2019) confirmed the current results, they found that the acute administration of CuO NPs is the main contributor in elevation of the liver function parameters after 14 days. The same results were obtained by Anreddy (2018), Abdelazeim et al. (2020), and Ghonimi et al. (2022) who confirmed the perturbation of the hepatic function by CuO NPs depending on the route, dose and time of administration. The key process of the hepatotoxicity by CuO NPs is the oxidative stress which matches with the current investigation that revealed marked reduction in the catalase and glutathione reductase activity. Further, the generation

of ROS is associated with undesirable modulation of the immune system which implicated in the damage of that defense mechanism, production of the proinflammatory cytokines as TNF- $\alpha$ , IL-1 $\beta$  and IL-6 ending with the liver injury, damage of the hepatocytes and apoptosis (Tulinska et al. (2022)). Here, the level of catalase and glutathione reductase enzymes in the liver homogenate markedly declined in dose-dependent manner that is agreed with the (Alarifi et al., 2013) and Anreddy (2018). In contrary with the current results, Srikanth et al. (2016) reported elevation of GSH by exposing the salmon cells to CuO NPs via in vitro study. Furthermore, It is postulated that there is an advanced link between the oxidative stress, genotoxicity and apoptosis (Shafagh et al., 2015). In addition, Asif et al. (2023) reported the potential antioxidant activity of CuO NPs by 2, 2'-azino-bis 3-ethyl benzthiazoline-6-sulfonic acid (ABTS), 2,2'-diphenyl-1-picrylhydrazyl (DPPH), hydrogen peroxide (H<sub>2</sub>O<sub>2</sub>) and superoxide radical (SOR) scavenging assays. Subsequently, the hepatocytes developed many adverse biological processes as cleavage of caspase-3, DNA fragmentation, breakdown of the cytoskeletal and nuclear protein, and formation of the granzymes (Martinvalet et al., 2005). Furthermore, the cell membrane contains carboxylic and amines group that enhances cross soluble copper ions intracellularly and accumulation of superoxide or hydroxyl radicals that leads to oxidative stress. Consequently, CuO NPs initiates powerful cytotoxicity by different mechanisms as DNA breakdown, mitochondrial destruction, ribosomes alteration and deterioration of cell membrane channels resulting in cell death and apoptosis (Camacho-Flores et al., 2015; Akintelu et al., 2020). The adverse effect of

the CuO NPs extended to the hepatic tissue, the current histological findings coincide with those reported by Abdelazeim et al. (2020) who found alteration in the hepatic architecture due to oxidative damage and suppression of the antioxidant activity. These histological changes are represented by the hepatic necrosis associated with the inflammatory cell infiltration and central vein dilatation. However, (Bugata et al., 2019) reported that the change in the hepatic histological structure is dose dependent thus they found no change in the low dose while the high dose showed severe necrosis inflammatory cell infiltration with severe dilatation of the central vein with obvious congestion.

Not only the liver but also kidney is considered the predominant organ for the Cu accumulation. Therefore, the kidney function and normal histological structure also altered after the oral administration specially in the higher dose. In the current study, the altered renal function parameters extremely elevated particularly at those 2000 mg/kg. On the cellular level, the oxidative stress induced by CuO NPs was implicated in renal deterioration. Copper oxide nanoparticles increased the level of MDA (Rodhe et al., 2015) and weakened antioxidant activity by downregulation of catalase and glutathione peroxidase 3 (Naz et al., 2020) confirming the current results. At the same time, cytotoxicity induced by ROS followed by genotoxicity, generation of ROS enhances the production of P53 and P83 proteins that damage DNA and apoptosis in addition to production of the inflammatory cytokines (Midander et al., 2009). Furthermore, administration of high dose of CuO NPs for long period is associated with disturbance of ions reabsorption and excretion. For instance, it's associated with the decline of the

potassium, sodium and chloride ions while elevation in urea and the creatinine levels (Elkhateeb et al., 2020). They reported histological changes and nephrotoxicity induced by CuO NPs where coincide with the results of Rodhe et al. (2015). They found necrosis of proximal convoluted tubules with atrophy and glomerulus at dose 200 mg/kg while, the lower dose 100 mg/kg showed slight swelling of the renal tubules. Moreover, (Lei et al., 2015) reported the swelling of the glomerulus and perturbation of the lumen of the Bowman's capsule indicating glomerulonephritis. In general, cytotoxicity of CuO NPs was studied in both *in vitro* in adenocarcinomic human alveolar basal epithelial cells (A549) and human hepatocellular carcinoma cells (HepG2). Potent generation of lipid peroxidation and ROS was observed after exposure to CuO NPs however, antioxidant status was recorded by lower glutathione (GSH) levels. Besides. Other literature mentioned that malondialdehyde (MDA), a lipid peroxidation marker and antioxidant enzymes like superoxide dismutase (SOD) and catalase (CAT), elevated markedly followed by reduction in glutathione (GSH) level (Sania Naz et al., 2023).

The limitation of the current study to investigate the rescue of the CuO NPs toxicity is owing to high mortality rate and the limitation of technical facilities that will be considered in the future study.

### **Conclusion**

This study endeavors to bridge the gap between overdose of CuO NPs and liver, kidney function associated with antioxidant status. All used doses of CuO NPs elevate liver function (AST, ALT and ALP), kidney function (urea and creatinine) parameters and antioxidant activity (catalase and glutathione reductase). The deleterious effect of CuO NPs was irreversible with

time after administration besides, undesirable effect was observed markedly at high dose (1000 and 2000 mg/kg).

### Reference

- Abdelazeim, S. A., Shehata, N. I., Aly, H. F., & Shams, S. G. E. (2020). Amelioration of oxidative stress-mediated apoptosis in copper oxide nanoparticles-induced liver injury in rats by potent antioxidants. *Scientific Reports*, 10(1), 10812. doi:10.1038/s41598-020-67784-y
- Akintelu, S. A., Folorunso, A. S., Folorunso, F. A., & Oyebamiji, A. K. (2020). Green synthesis of copper oxide nanoparticles for biomedical application and environmental remediation. *Heliyon*, 6(7), e04508. doi:10.1016/j.heliyon.2020.e04508
- Alarifi, S., Ali, D., Verma, A., Alakhtani, S., & Ali, B. A. (2013). Cytotoxicity and genotoxicity of copper oxide nanoparticles in human skin keratinocytes cells. *Int J Toxicol*, 32(4), 296-307. doi:10.1177/1091581813487563
- Ameh, T., & Sayes, C. M. (2019). The potential exposure and hazards of copper nanoparticles: A review. *Environ Toxicol Pharmacol*, 71, 103220. doi:10.1016/j.etap.2019.103220
- Anreddy, R. N. R. (2018). Copper oxide nanoparticles induces oxidative stress and liver toxicity in rats following oral exposure. *Toxicology reports*, 5, 903-904. doi:10.1016/j.toxrep.2018.08.022
- Asbrink, S., & Waskowska, A. (1991). CuO: X-ray single-crystal structure determination at 196 K and room temperature. *Journal of Physics Condensed Matter*, 3, 8173-8180. doi:10.1088/0953-8984/3/42/012
- Asif, N., Ahmad, R., Fatima, S., Shehzadi, S., Siddiqui, T., zaki, A., & Fatma, T. (2023). Toxicological assessment of Phormidium sp. derived copper oxide nanoparticles for its biomedical and environmental applications. *Scientific Reports*, 13(1), 6246. doi:10.1038/s41598-023-33360-3
- Bhattacharya, P. T., Misra, S. R., & Hussain, M. (2016). Nutritional Aspects of Essential Trace Elements in Oral Health and Disease: An Extensive Review. *Scientifica*, 2016, 5464373. doi:10.1155/2016/5464373
- Bugata, L. S. P., Pitta Venkata, P., Gundu, A. R., Mohammed Fazlur, R., Reddy, U. A., Kumar, J. M., . . . Mahboob, M. (2019). Acute and subacute oral toxicity of copper oxide nanoparticles in female albino Wistar rats. *Journal of Applied Toxicology*, 39(5), 702-716. doi:<https://doi.org/10.1002/jat.3760>
- Camacho-Flores, B., Martínez-Álvarez, O., Arenas-Arrocena, M., Garcia-Contreras, R., Argueta-Figueroa, L., De La Fuente-Hernández, J., & Acosta-Torres, L. (2015). Copper: synthesis techniques in nanoscale and powerful application as an antimicrobial agent. *Journal of Nanomaterials*, 16(1), 423-423.
- Chen, Z., Meng, H., Xing, G., Chen, C., Zhao, Y., Jia, G., . . . Wan, L. (2006). Acute toxicological effects of copper nanoparticles in vivo. *Toxicol Lett*, 163(2), 109-120. doi:10.1016/j.toxlet.2005.10.003
- Chithrani, B. D., Ghazani, A. A., & Chan, W. C. (2006). Determining the size and shape dependence of gold nanoparticle uptake into mammalian cells. *Nano Lett*, 6(4), 662-668. doi:10.1021/nl052396o

- Dagher, S., Haik, Y., Ayesh, A. I., & Tit, N. (2014). Synthesis and optical properties of colloidal CuO nanoparticles. *Journal of Luminescence*, 151, 149-154. doi:<https://doi.org/10.1016/j.jlumin.2014.02.015>
- El Bialy, B. E., Hamouda, R. A., Abd Eldaim, M. A., El Ballal, S. S., Heikal, H. S., Khalifa, H. K., & Hozzein, W. N. (2020). Comparative Toxicological Effects of Biologically and Chemically Synthesized Copper Oxide Nanoparticles on Mice. *Int J Nanomedicine*, 15, 3827-3842. doi:10.2147/ijn.S241922
- Elkhateeb, S. A., Ibrahim, T. R., El-Shal, A. S., & Abdel Hamid, O. I. (2020). Ameliorative role of curcumin on copper oxide nanoparticles-mediated renal toxicity in rats: An investigation of molecular mechanisms. *J Biochem Mol Toxicol*, 34(12), e22593. doi:10.1002/jbt.22593
- Gaetke, L. M., Chow-Johnson, H. S., & Chow, C. K. (2014). Copper: toxicological relevance and mechanisms. *Arch Toxicol*, 88(11), 1929-1938. doi:10.1007/s00204-014-1355-y
- Gamble, M. (2008). 9 - The Hematoxylin and Eosin. In J. D. Bancroft & M. Gamble (Eds.), *Theory and Practice of Histological Techniques* (Sixth Edition) (pp. 121-134). Edinburgh: Churchill Livingstone.
- Ghonimi, W. A. M., Alferah, M. A. Z., Dahran, N., & El-Shetry, E. S. (2022). Hepatic and renal toxicity following the injection of copper oxide nanoparticles (CuO NPs) in mature male Westar rats: histochemical and caspase 3 immunohistochemical reactivities. *Environmental Science and Pollution Research*, 29(54), 81923-81937. doi:10.1007/s11356-022-21521-2
- Grigore, M., Biscu, E., Holban, A., Gestal, M., & Grumezescu, A. (2016). Methods of Synthesis, Properties and Biomedical Applications of CuO Nanoparticles. *Pharmaceuticals*, 9(4), 75. doi:10.3390/ph9040075
- Hasan, I. M. A., Tawfik, A. R., & Assaf, F. H. (2021). Biosynthesis of  $\alpha$ -MoO<sub>3</sub> nanoparticles and its adsorption performance of cadmium from aqueous solutions. *Advances in Natural Sciences: Nanoscience and Nanotechnology*, 12(3), 035007. doi:10.1088/2043-6262/ac2050
- Hasan, I. M. A., Tawfik, A. R., & Assaf, F. H. (2022). GC/MS screening of buckthorn phytochemicals and their use to synthesize ZnO nanoparticles for photocatalytic degradation of malachite green dye in water. *Water Sci Technol*, 85(2), 664-684. doi:10.2166/wst.2021.638
- He, H., Zou, Z., Wang, B., Xu, G., Chen, C., Qin, X., . . . Zhang, J. (2020). Copper Oxide Nanoparticles Induce Oxidative DNA Damage and Cell Death via Copper Ion-Mediated P38 MAPK Activation in Vascular Endothelial Cells. *International Journal of Nanomedicine*, Volume 15, 3291-3302. doi:10.2147/ijn.s241157
- Kim, J. H., Kim, J. H., Kim, K. W., Kim, M. H., & Yu, Y. S. (2009). Intravenously administered gold nanoparticles pass through the blood-retinal barrier depending on the particle size, and induce no retinal toxicity. *Nanotechnology*, 20(50), 505101. doi:10.1088/0957-4484/20/50/505101

- Kittel, B., Ruehl-Fehlert, C., Morawietz, G., Klapwijk, J., Elwell, M. R., Lenz, B., . . . Wadsworth, P. F. (2004). Revised guides for organ sampling and trimming in rats and mice--Part 2. A joint publication of the RITA and NACAD groups. *Exp Toxicol Pathol*, 55(6), 413-431. doi:10.1078/0940-2993-00349
- Lateef, R., Marhaba, Mandal, P., Ansari, K. M., Javed Akhtar, M., & Ahamed, M. (2023). Cytotoxicity and apoptosis induction of copper oxide-reduced graphene oxide nanocomposites in normal rat kidney cells. *Journal of King Saud University - Science*, 35(2), 102513. doi:<https://doi.org/10.1016/j.jksus.2022.102513>
- Lee, I. C., Ko, J. W., Park, S. H., Lim, J. O., Shin, I. S., Moon, C., . . . Kim, J. C. (2016). Comparative toxicity and biodistribution of copper nanoparticles and cupric ions in rats. *Int J Nanomedicine*, 11, 2883-2900. doi:10.2147/ijn.S106346
- Lei, R., Yang, B., Wu, C., Liao, M., Ding, R., & Wang, Q. (2015). Mitochondrial dysfunction and oxidative damage in the liver and kidney of rats following exposure to copper nanoparticles for five consecutive days. *Toxicology Research*, 4(2), 351-364.
- Martinvalet, D., Zhu, P., & Lieberman, J. (2005). Granzyme A induces caspase-independent mitochondrial damage, a required first step for apoptosis. *Immunity*, 22(3), 355-370. doi:10.1016/j.immuni.2005.02.004
- Maulana, I., Fasya, D., & Ginting, B. (2022). Biosynthesis of Cu nanoparticles using *Polyalthia longifolia* roots extracts for antibacterial, antioxidant and cytotoxicity applications. *Materials Technology*, 37(13), 2517-2521. doi:10.1080/10667857.2022.2044217
- Midander, K., Cronholm, P., Karlsson, H. L., Elihn, K., Möller, L., Leygraf, C., & Wallinder, I. O. (2009). Surface characteristics, copper release, and toxicity of nano- and micrometer-sized copper and copper(II) oxide particles: a cross-disciplinary study. *Small*, 5(3), 389-399. doi:10.1002/sml.200801220
- Naz, S., Gul, A., & Zia, M. (2020). Toxicity of copper oxide nanoparticles: a review study. *IET Nanobiotechnol*, 14(1), 1-13. doi:10.1049/iet-nbt.2019.0176
- Naz, S., Gul, A., Zia, M., & Javed, R. (2023). Synthesis, biomedical applications, and toxicity of CuO nanoparticles. *Applied Microbiology and Biotechnology*, 107(4), 1039-1061. doi:10.1007/s00253-023-12364-z
- OECD. (2001). OECD GUIDELINE FOR TESTING OF CHEMICALS. OECD/OCDE, Adopted 17th December; 1-14.
- Osredkar, J., & Sustar, N. (2011). Copper and zinc, biological role and significance of copper/zinc imbalance. *J Clin Toxicol S*, 3(2161), 0495.
- Rodhe, Y., Skoglund, S., Odnevall Wallinder, I., Potáčová, Z., & Möller, L. (2015). Copper-based nanoparticles induce high toxicity in leukemic HL60 cells. *Toxicol In Vitro*, 29(7), 1711-1719. doi:10.1016/j.tiv.2015.05.020
- Schipper, M. L., Iyer, G., Koh, A. L., Cheng, Z., Ebenstein, Y., Aharoni,

- A., Gambhir, S. S. (2009). Particle size, surface coating, and PEGylation influence the biodistribution of quantum dots in living mice. *Small*, 5(1), 126-134.
- Shafagh, M., Rahmani, F., & Delirez, N. (2015). CuO nanoparticles induce cytotoxicity and apoptosis in human K562 cancer cell line via mitochondrial pathway, through reactive oxygen species and P53. *Iran J Basic Med Sci*, 18(10), 993-1000.
- Srikanth, K., Pereira, E., Duarte, A. C., & Rao, J. V. (2016). Evaluation of cytotoxicity, morphological alterations and oxidative stress in Chinook salmon cells exposed to copper oxide nanoparticles. *Protoplasma*, 253(3), 873-884. doi:10.1007/s00709-015-0849-7
- Taton, T. A. (2002). Nanostructures as tailored biological probes. *Trends in Biotechnology*, 20(7), 277-279. doi:[https://doi.org/10.1016/S0167-7799\(02\)01973-X](https://doi.org/10.1016/S0167-7799(02)01973-X)
- Thommes, M., Kaneko, K., Neimark, A. V., Olivier, J. P., Rodriguez-Reinoso, F., Rouquerol, J., & Sing, K. S. W. (2015). Physisorption of gases, with special reference to the evaluation of surface area and pore size distribution (IUPAC Technical Report). *Pure and Applied Chemistry*, 87(9-10), 1051-1069. doi:10.1515/pac-2014-1117
- Tulinska, J., Mikusova, M. L., Liskova, A., Busova, M., Masanova, V., Uhnakova, I., . . . Mikuska, P. (2022). Copper Oxide Nanoparticles Stimulate the Immune Response and Decrease Antioxidant Defense in Mice After Six-Week Inhalation. *Frontiers in Immunology*, 13. doi:10.3389/fimmu.2022.874253
- Usman, M. S., El Zowalaty, M. E., Shameli, K., Zainuddin, N., Salama, M., & Ibrahim, N. A. (2013). Synthesis, characterization, and antimicrobial properties of copper nanoparticles. *Int J Nanomedicine*, 8, 4467-4479. doi:10.2147/ijn.S50837
- Vinothkanna, A., Mathivanan, K., Ananth, S., Ma, Y., & Sekar, S. (2022). Biosynthesis of copper oxide nanoparticles using *Rubia cordifolia* bark extract: characterization, antibacterial, antioxidant, larvicidal and photocatalytic activities. *Environ Sci Pollut Res Int*. doi:10.1007/s11356-022-18996-4
- Waris, A., Din, M., Ali, A., Ali, M., Afridi, S., Baset, A., & Ullah Khan, A. (2021). A comprehensive review of green synthesis of copper oxide nanoparticles and their diverse biomedical applications. *Inorganic Chemistry Communications*, 123, 108369. doi:<https://doi.org/10.1016/j.inoche.2020.108369>